Journal of Alloys and Compounds 525 (2012) 114–119

Contents lists available at SciVerse ScienceDirect

Journal of Alloys and Compounds

journal homepage: www.elsevier.com/locate/jallcom

Effect of Nd–Co substitution on magnetic and microwave absorption properties of $SrFe_{12}O_{19}$ hexaferrites

Zeyang Zhang[a], Xiangxuan Liu[a,*], Xuanjun Wang[a], Youpeng Wu[b], Rong Li[a]

[a] No. 503 Faculty, Xi'an Research Institute of High Technology, Xi'an 710025, China
[b] Beijing Research Institute of High Technology, Beijing 100085, China

ARTICLE INFO

Article history:
Received 29 November 2011
Received in revised form 8 February 2012
Accepted 13 February 2012
Available online xxx

Keywords:
Nd–Co substitution
Strontium ferrites
Magnetic properties
Microwave absorption

ABSTRACT

Nd–Co-substituted M-type strontium hexaferrites were prepared by sol–gel-autocombustion method. Crystalline structure, morphology, magnetic properties, and microwave absorption properties of $Sr_{1-x}Nd_xFe_{12-x}Co_xO_{19}$ (x = 0–0.4) were studied via X-ray diffraction, scanning electron microscope, vibrating sample magnetometer, and vector network analyzer, respectively. Single-phase M-type strontium hexaferrites, with a chemical composition of $Sr_{1-x}Nd_xFe_{12-x}Co_xO_{19}$ (x = 0–0.3), were formed by being heated at 1200 °C for 3 h in air. Saturation magnetization and coercivity reached a maximum at x = 0.2. For samples with x = 0.2, a minimum reflection loss of −22 dB was obtained at 16.2 GHz for a layer of 1.9 mm in thickness. The reflection loss of $Sr_{0.8}Nd_{0.2}Fe_{11.8}Co_{0.2}O_{19}$ ferrite (1.5–3.0 mm in thickness) is less than −10 dB over the range of 9.8–18 GHz. It indicates that the substituted Nd–Co can greatly improve the microwave absorption properties of $SrFe_{12}O_{19}$ hexaferrites.

1. Introduction

Microwave-absorbing materials have gained increasing attention due to the prevalence of electromagnetic interference problems and because these materials are an essential part of stealth defense systems for all military technologies [1–5]. The absorbent is the core of an absorbing material. Thus, extensive studies on microwave absorption properties of various materials have been investigated to select a suitable absorbent with high absorptive ability and wide band absorption. The most current research focuses on using ZnO composites [4–7], carbon nanotubes [8,9], ferrites [10,3,11], metal alloys [12] and so on, as absorbents. M-type ferrites have been widely used as microwave attenuation materials and have recently received considerable attention from researchers [13–17] because of their large anisotropy field, high saturation magnetization, and excellent chemical stability. Many studies have been recently carried out to investigate the influence of rare earth substitution on magnetic and microwave absorption properties of ferrite materials [18–20]. Using rare earth as dopants has been reported as an effective method in varying magnetic and microwave absorption properties of ferrite materials. Li et al. [20] have revealed that La-substituted barium ferrite exhibited excellent microwave absorption properties compared with pure barium ferrite. The bandwidth below −10 dB expands from 0 GHz to 12.6 GHz and the peak value of reflection loss decreases from −9.65 dB to −23.02 dB with the layer thickness of 2.0 mm. Several researchers have reported that La–Co and Nd–Co substitution in M-type ferrites prepared using chemical coprecipitation was effective in improving magnetic properties of the ferrites [21–23]. However, only a few studies have been conducted on the microwave absorption properties of Nd–Co-substituted M-type strontium hexaferrites.

In the present study, Nd–Co-substituted M-type hexaferrites were prepared by sol–gel-autocombustion method. Sublattice structure, magnetic, electromagnetic, and microwave absorption properties of Nd–Co-substituted M-type hexaferrites were investigated. In addition, the relationships among these properties were also investigated.

2. Experimental

2.1. Synthesis of $Sr_{1-x}Nd_xFe_{12-x}Co_xO_{19}$ hexaferrite

Sr–Nd–Co hexagonal ferrites were prepared by sol–gel-autocombustion method. According to $Sr_{1-x}Nd_xFe_{12-x}Co_xO_{19}$ (x = 0, 0.1, 0.2, 0.3, 0.4), stoichiometric amounts of strontium nitrate, cobalt nitrate, neodymium nitrate, and iron nitrate were dissolved in deionized water, and then the proper amount of citric acid was added to complex the metal ions completely. The molar ration of citric acid and NO_3 ions was controlled as 1:1. The pH value of the sol was adjusted to 6.0 using ammonia solution (25 wt%). The solution was evaporated at 80 °C until a viscous gel formed. Then, it was dried into dry gel at 120 °C. The dry gel was ignited in air and burned into dendritic powders. Finally, the precursor powder was sintered at 1200 °C for 3 h.

* Corresponding author. Tel.: +86 15902957276; fax: +86 02983348220.
E-mail address: xiangxuan_study@yahoo.com (X. Liu).

0925-8388/$ – see front matter © 2012 Elsevier B.V. All rights reserved.
doi:10.1016/j.jallcom.2012.02.088

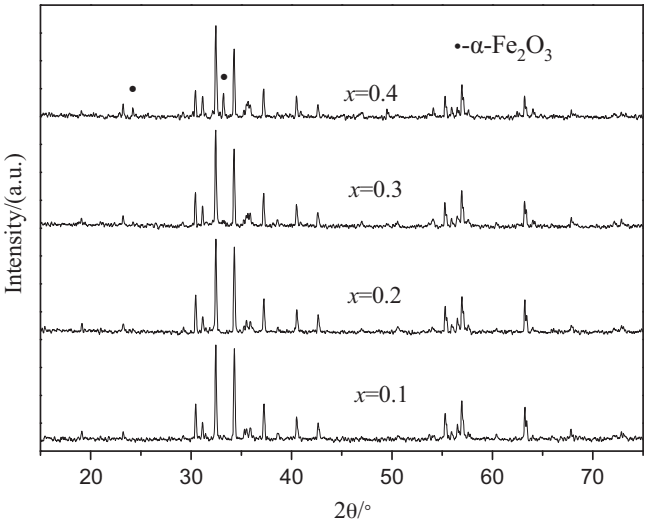

Fig. 1. XRD patterns of $Sr_{1-x}Nd_xFe_{12-x}Co_xO_{19}$ M-type ferrite fine particles.

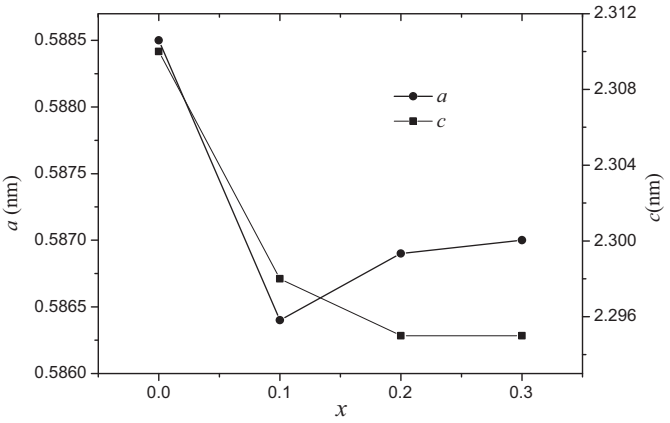

Fig. 2. Variation of lattice parameters (a and c) as a function of x.

2.2. Preparation of composites plates

Sr–Nd–Co hexagonal ferrites powders were dispersed into an epoxide resin by solvent addition and using a high energy ultrasonic treatment for 30 min. A hardener was then added into the mixtures, followed by stirring at 1000 rpm for 10 min. Finally, the composite materials were fabricated on an aluminum substrate with a standard size (180 mm × 180 mm × 3 mm). The thickness of the composite materials was controlled using different thickness models.

2.3. Measurement, analysis methods of properties and structure

The resulting crystalline phases were characterized using X-ray diffraction (XRD; D/max–IIB, Japan). Data were recorded using Cu K_α radiation at 40.0 kV and 100.0 mA in the 2θ region, from 15° to 70°, with a scanning speed of 15°/min. The magnetic properties were investigated using a vibrating sample magnetometer (VSM, Lakeshore, Model 7300 series). A VEGA II XMU INCA scanning electron microscope (SEM) was employed for morphological analysis. The EM parameters (complex permeability and permittivity) were measured using a vector network analyzer (HP-8720ES) in the frequency range of 2–18 GHz. The samples used for EM parameter measurement were prepared by dispersing powders into paraffin wax with mass fraction of 60%, and then pressing the mixtures into a compact toroidal shape. The reflection loss of the prepared absorbers versus frequency was studied using an HP 8510B vector network analyzer and standard horn antennas in an anechoic chamber.

3. Results and discussion

3.1. Crystalline structure analysis

Fig. 1 shows the XRD patterns of $Sr_{1-x}Nd_xFe_{12-x}Co_xO_{19}$, with $x = 0$, 0.1, 0.2, 0.3 and 0.4. The samples were all annealed at 1200 °C for 3 h. Patterns corresponding to pure hexagonal ferrite phase appear in the samples, with $x \leq 0.3$. When $x = 0.4$, the phases of a-Fe_2O_3 appear. These indicate that the substitution amount cannot overpass 0.4. Using d-spacing values, lattice parameters a and c were calculated using the following equation and the results are given in Fig. 2.

$$d_{hkl} = \left(\frac{4(h^2 + hk + k^2)}{3a^2} + \left(\frac{l}{c} \right)^2 \right)^{-1/2} \quad (1)$$

It can be seen that lattice parameter a for the samples first increased and then decreased with an increase in x value. Lattice parameter c decreases slightly with an increase in x value, but the difference is imperceptible. This may be explained by the compensation of the difference in ionic radii between Nd^{3+} ion (0.115 nm) and Sr^{2+} ion (0.127 nm), and between Co^{2+} ion (0.0745 nm) and Fe^{3+} ion (0.0645 nm) [24,25]. Thus, a competition between the increase and decrease in the lattice parameters occurs, thereby causing irregular changes in a as well as a decrease in c.

3.2. SEM analysis

Fig. 3 shows SEM images for the samples with various substitution amounts prepared at 1200 °C for 3 h in air. It is shown that the grain shape is platelet-like. The grain size of typical particles decreases with the increase in x when the amount of substitution ranged from $x = 0.1$ to $x = 0.4$. The decreasing trend of the grain size with increasing rare earth element Nd^{3+} concentration shows that Nd^{3+} acts as a grain growth inhibitor, which is in accordance with the literatures [26,27].

Fig. 4(a) and (b) are the surface and section SEM observation, respectively, which show the microstructure of the coating filled with 60% doped strontium hexagonal ferrites. It can be observed that the fillers are well dispersed in the epoxide resin matrix and no significant porosity was noticed.

3.3. Magnetic properties

Saturation magnetization (M_s) and coercive force (H_c) of the prepared samples were measured via VSM at a maximum applied field of 10,000 Oe at room temperature. The effects of different substitution amounts of Nd–Co on magnetic properties of strontium ferrite powder are shown in Figs. 5 and 6.

It can be found that the suitable amount of Nd–Co substitution may remarkably increase saturation magnetization. As shown in Fig. 5, M_s for the samples first increased and then decreased with an increase in the Nd–Co substitution amounts. M_s for samples without substitution at ($x = 0$) is 48 Am^2/kg. At $x = 0.1$, the value of M_s is 53 Am^2/kg, and at $x = 0.2$, M_s increases to a maximum value of 58 Am^2/kg. At $x = 0.3$ and 0.4, M_s decreases with a further increase in substitution amounts. In M-type hexagonal ferrites, the unit cell consists of two molecules. Within the basic structure, Fe^{3+} ions occupy five different interstitial sites, namely, tetrahedral $4f_1$ (↓), bipyramidal 2b (↑), and three octahedral sites [12 K (↑), $4f_2$ (↓), and 2a (↑)], where ↑ and ↓ denote the spin orientations of Fe^{3+} ions at the different sites, and the number in the expression indicates the number of Fe^{3+} ions per unit cell. This magnetic behavior of the substituted samples may depend upon the following factors. Magnetic of ferrous magnetic material derived from the sub-lattice spin-up and spin-down the difference between the magnetic moment. Most of the Co^{2+} is substituted for Fe^{3+} in the octahedral $4f_2$ (↓) and 2a (↑) sites, and a valence change of some Fe^{3+} to Fe^{2+} occurs in the

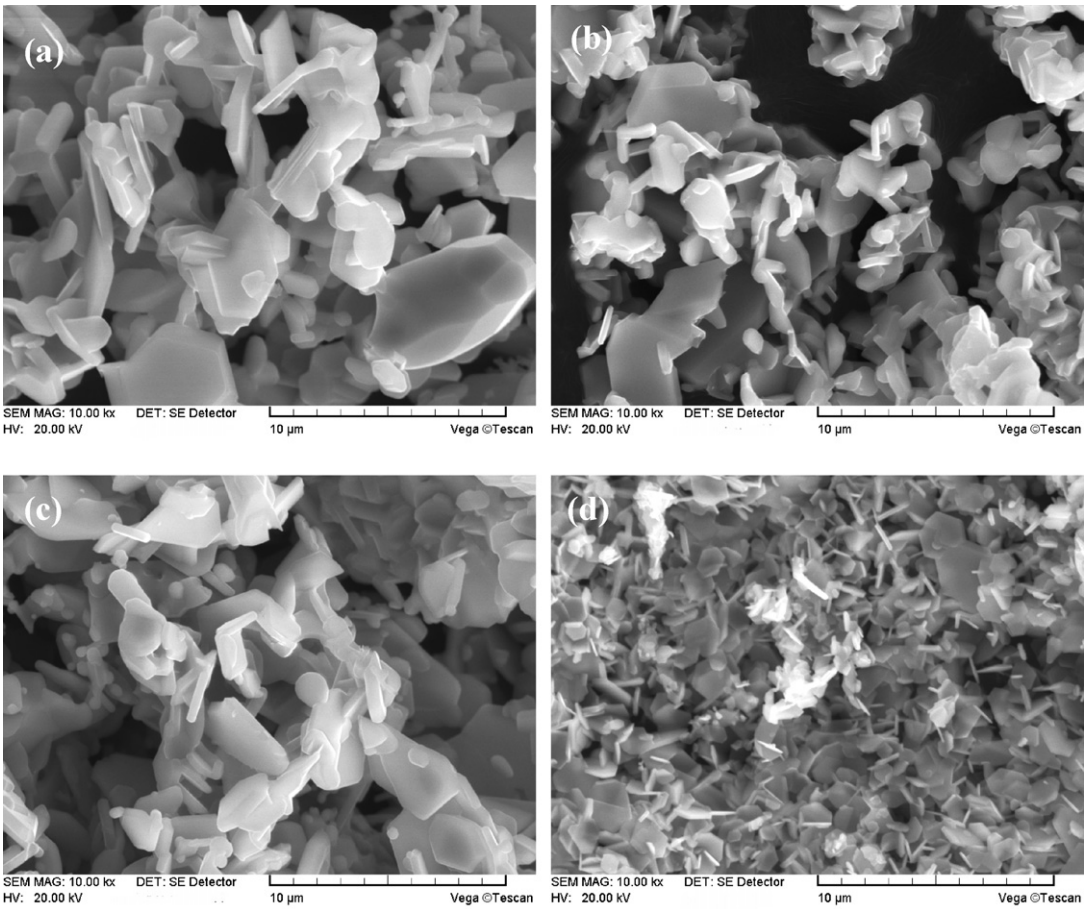

Fig. 3. SEM micrograph for powder samples with various amounts of $Sr_{1-x}Nd_xFe_{12-x}Co_xO_{19}$ (a) $x = 0.1$, (b) $x = 0.2$, (c) $x = 0.3$ and (d) $x = 0.4$.

2a sites. Mässbauer investigations show that Co^{2+} ion is randomly distributed in the $4f_2$ (↓) and 2a (↑) sites [28–31]. The magnetic moment of Co^{2+} (~3.7 μ_B) is smaller than Fe^{3+} (~5 μ_B). When the substitution amount $x \leq 0.2$, the substitution amount of Co^{2+} in the spin-down $4f_2$ site is more than in the spin-up 2a site, which leads to an increase in molar magnetic moment. When x equal to 0.3, the substitution amount of Co^{2+} in the spin-up 2a site increase and some Fe^{3+} ions in the 2a site change to Fe^{2+}, which lead to a decrease in molar magnetic moment. When x is larger than 0.4, the nonmagnetic impurities (a-Fe_2O_3) result into more decreasing of saturation magnetization. Therefore, maximal magnetization increases with an increase in x until $x = 0.2$ and then decreases.

As shown in Fig. 6, when there is no substitution of Nd–Co, the value of H_c is 262.7 kA/m. A decrease in the coercive force was observed with the substitution of Nd–Co for $x = 0$–0.1. Further increase in Nd–Co substitution ($x = 0.2$) results in an increase of the coercive force up to 302.5 kA/m. However, as Nd–Co content increases, a steady decrease in coercive force is consequently observed for $x = 0.3$ ($H_c = 191.1$ kA/m) and for $x = 0.4$ ($H_c = 159.2$ kA/m).

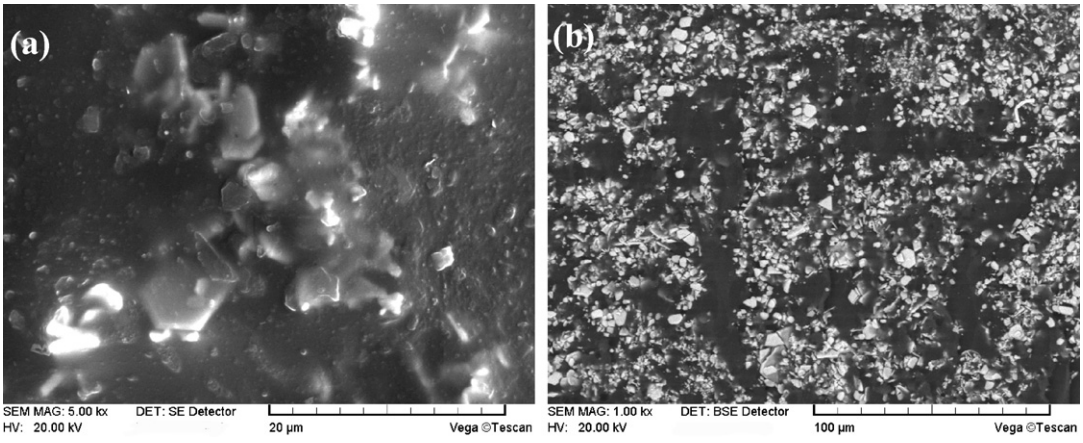

Fig. 4. SEM micrograph of microstructure of coating surface and section.

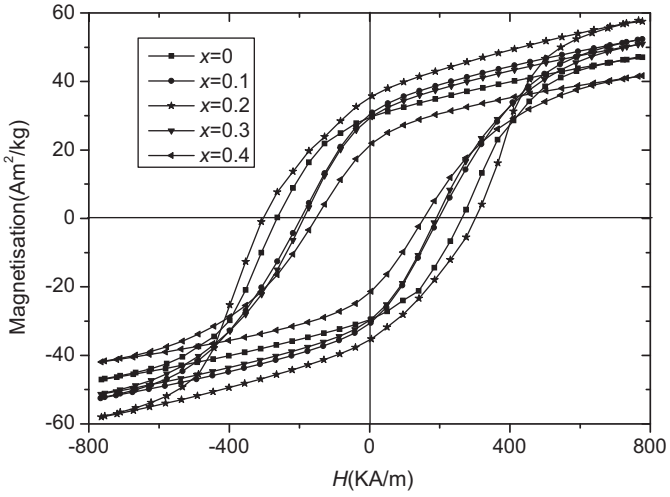

Fig. 5. Hysteresis loops of $Sr_{1-x}Nd_xFe_{12-x}Co_xO_{19}$ ($x = 0.0$–0.4).

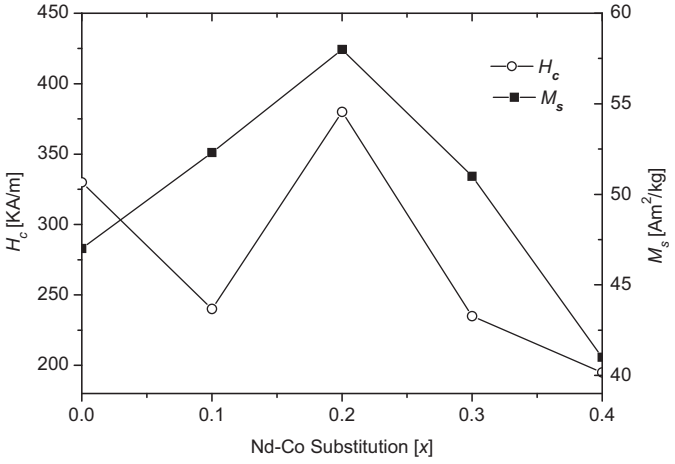

Fig. 6. Variation of saturated magnetization and coercive force with Nd–Co substitution in M-type hexaferrites.

3.4. Complex permittivity and permeability of Nd–Co-doped strontium ferrite

Complex permittivity and permeability represent the dielectric and the dynamic magnetic properties of materials. Complex permittivity and permeability of the composite filled with 60% $Sr_{1-x}Nd_xFe_{12-x}Co_xO_{19}$ powders are shown in Fig. 7. For the samples with $x = 0.1$, 0.2 and 0.3, the real and imaginary parts of permittivity are almost constant throughout measured frequency range and the values are higher as compared with the undoped one. When the substitution amount $x \leq 0.2$, the substitution amount make the real and imaginary parts of permittivity increasing. However, with the further increase of x, real and imaginary parts of permittivity become lower. The reason for this difference in

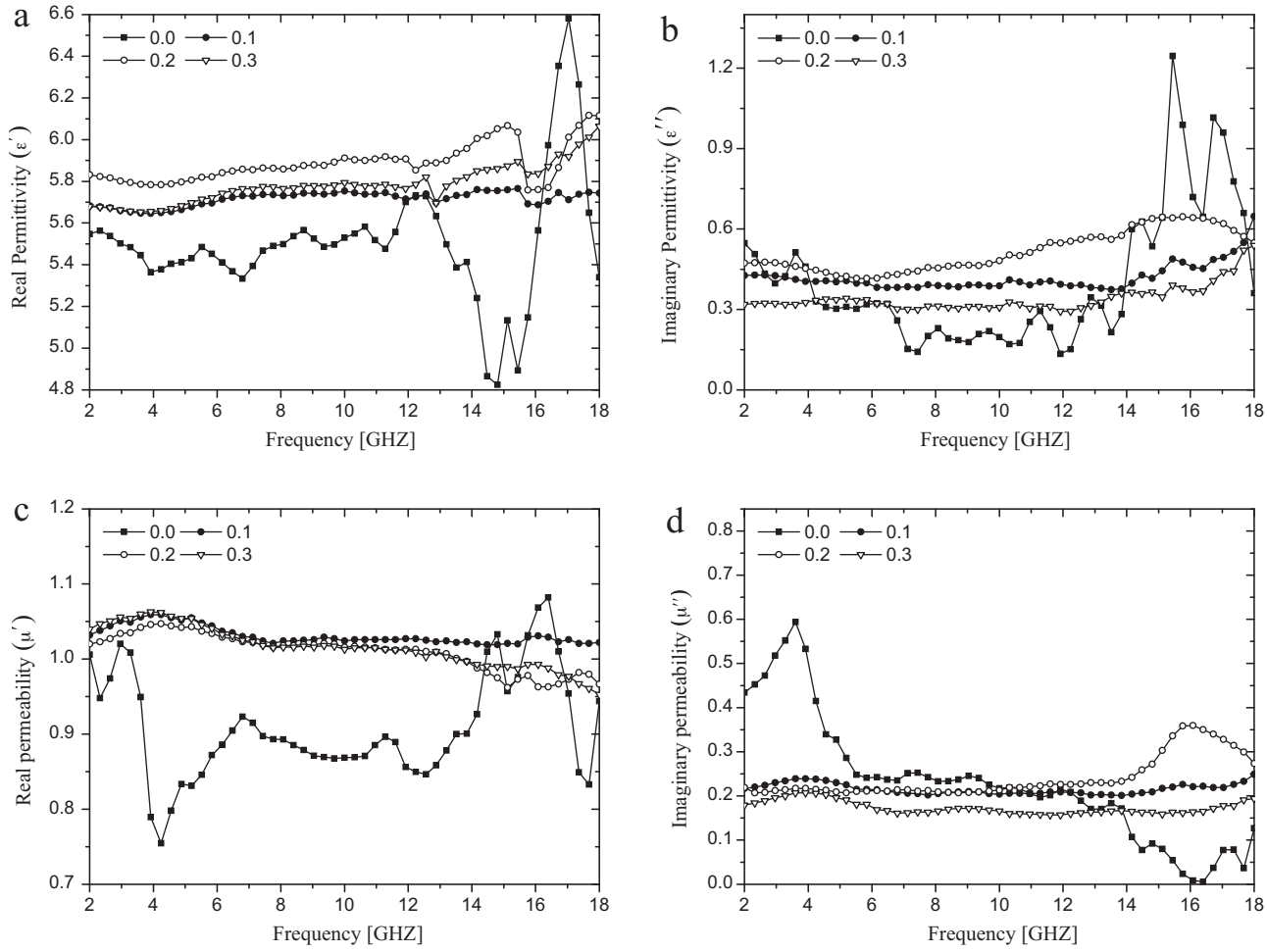

Fig. 7. Complex permeability and permittivity of composite samples containing $Sr_{1-x}Nd_xFe_{12-x}Co_xO_{19}$ powders.

complex permittivity of strontium hexagonal ferrites may be attributed to the significant contributions of Nd^{3+} and Co^{2+} ions. The dielectric properties of strontium hexagonal ferrites arise mainly due to the interfacial polarization and intrinsic electric dipole polarization. The electrons dipole polarization occurs as a consequence of the electrons hopping between ions with different valences. Thus, Nd^{3+} ions preferentially substitute Sr^{2+} ions, and Co^{2+} ions preferentially substitute Fe^{3+} ions, which will enhance the electron hopping.

Generally, for ferrite magnetic materials, the microwave magnetic loss mainly originates from domain wall resonance and natural ferromagnetic resonance [32]. Domain wall resonance usually occurs in the low-frequency region (<2 GHz). However, resonance due to the spin rotational component occurs at high-frequency regions. Thus, the magnetic loss in the M-type strontium hexaferrite-paraffin mixture should mainly arise from natural resonance. In samples with higher coercive force, natural resonance is observed in the frequency region of 2–18 GHz, as shown in Figs. 7(c) and 5(d). Resonance frequency was determined to be 3.5 and 16 GHz for samples with $x = 0$ and $x = 0.2$, respectively. With the weakening of uniaxial anisotropy (small coercive force), resonance frequency moves to a lower frequency region. For the samples with $x = 0.1$ and $x = 0.3$, no magnetic resonance is observed in the frequency range of 2–18 GHz. Natural resonance is believed to occur at a frequency below 2 GHz because of its small anisotropy field. The result is consistent with the ferromagnetic resonance theory, which states that if coercivity can be taken as the degree of the anisotropy field, resonance frequency is considered to be proportional to saturated magnetization and coercivity [33,34].

3.5. Microwave characteristics

The normalized input impedance, Z_{in}, of a metal-backed microwave absorption layer could be obtained from the following expression [35]:

$$Z_{in} = Z_0 \left(\frac{\mu_r}{\varepsilon_r}\right)^{1/2} \tanh\left[\frac{j2\pi df\sqrt{\varepsilon_r\mu_r}}{c}\right] \quad (2)$$

where $Z_0 = \sqrt{\mu_0/\varepsilon_0} = 377\Omega$ is the intrinsic impedance of free space, f is the frequency of the EM wave, d is the thickness of an absorber, and c is the velocity of light in vacuum.

According to the transmission line theory, reflection loss (RL) is a function of the reflection coefficient and can be expressed as follows [36]:

$$\mathrm{RL} = 20\log\left|\frac{Z_{in} - Z_0}{Z_{in} + Z_0}\right| \quad (3)$$

The frequency versus reflection loss of the strontium hexagonal ferrites with different substitution amounts at layer thickness of 2.0 mm were calculated based on Eqs. (2) and (3) and shown in Fig. 8, respectively. It can be observed when the substitution amount $x \leq 0.2$, the substitution amount makes the minimum reflection loss decreasing. However, with the further increase of x, the microwave absorbing property becomes worse. $Sr_{0.8}Nd_{0.2}Fe_{11.8}Co_{0.2}O_{19}$ ferrite exhibits the best microwave absorption. According to literature [37], there are two fundamental conditions that must be satisfied to achieve low reflection. First, electromagnetic wave can enter into absorbing materials at the greatest extent (impedance matching characteristic). Second, electromagnetic wave entering into the materials can be almost entirely attenuated (attenuation characteristic). The second condition is more important than the first for ferrites materials. According to the second condition, the attenuation constant can be expressed as:

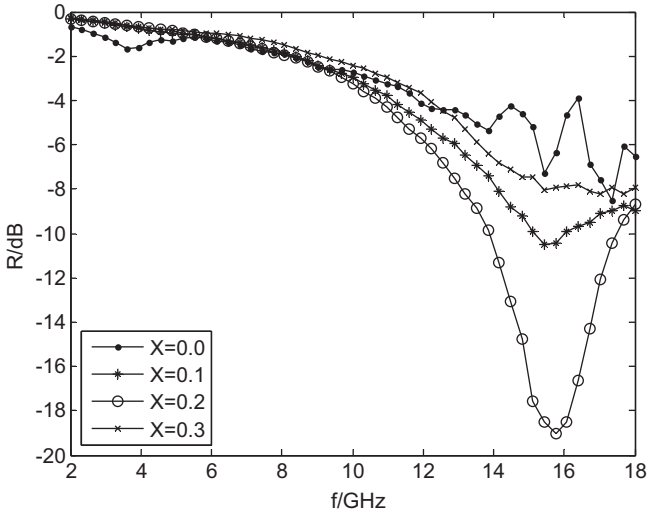

Fig. 8. Frequency dependences of reflection loss for $Sr_{1-x}Nd_xFe_{12-x}Co_xO_{19}$ ferrites at $d = 2$ mm.

$$\alpha = \frac{\sqrt{2}\pi f}{c} \times \sqrt{(\mu''\varepsilon'' - \mu'\varepsilon') + \sqrt{(\mu''\varepsilon'' - \mu'\varepsilon')^2 + (\varepsilon'\mu'' - \mu'\varepsilon'')^2}} \quad (4)$$

Fig. 9 shows the attenuation constants of strontium hexagonal ferrites with different substitution amounts. The attenuation constants of doped strontium hexagonal ferrites are higher than undoped one. The change trend of the attenuation constant of doped strontium hexagonal ferrites is in accordance with the microwave absorption in Fig. 8. When the substitution amount $x = 0.2$, the highest attenuation constant reach was obtained, which is in accordance with the microwave absorption. The substitution of Nd–Co improves the microwave attenuation ability of strontium hexagonal ferrites.

In order to study the microwave absorption performance of $Sr_{0.8}Nd_{0.2}Fe_{11.8}Co_{0.2}O_{19}$ ferrite, the relationship between reflection loss and frequency at different thicknesses was calculated and shown in Fig. 10. The reflection loss is greatly dependent on the thickness of coating. The peak of reflection loss shifts to lower frequency range with thickness increasing. The absorption property increases with the thickness and reaches a minimum at

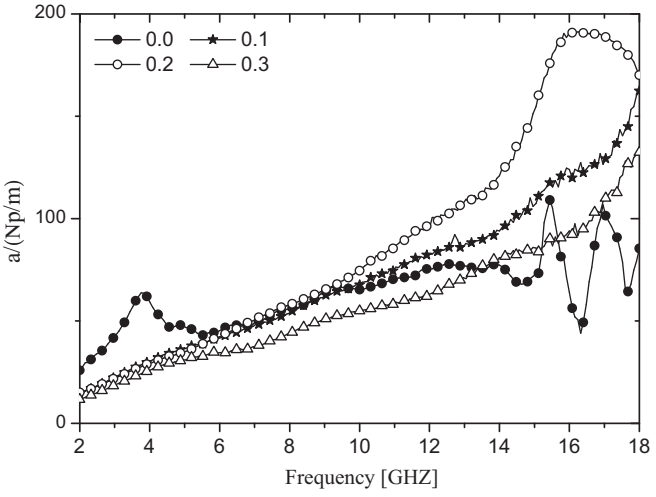

Fig. 9. Attenuation constant of $Sr_{1-x}Nd_xFe_{12-x}Co_xO_{19}$ powders.

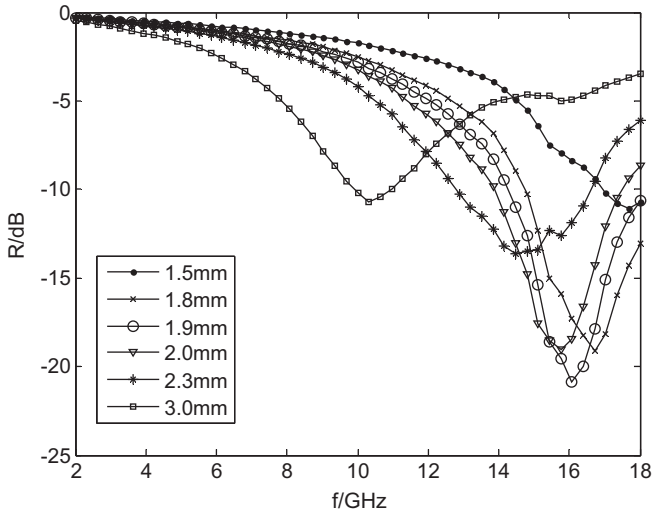

Fig. 10. Microwave absorbing properties of $Sr_{0.8}Nd_{0.2}Fe_{11.8}Co_{0.2}O_{19}$ ferrite with different thicknesses.

1.9 mm, whereas the reflection loss dramatically decreases when the thickness of coating exceeds 1.9 mm. The lowest reflection loss of $Sr_{0.8}Nd_{0.2}Fe_{11.8}Co_{0.2}O_{19}$ ferrite is −22 dB at 16.2 GHz and the corresponding thickness is 1.9 mm. The −10 dB absorption bandwidth corresponds to 68% EM wave amplitude attenuation or to 90% power attenuation. The results show that the reflection loss of $Sr_{0.8}Nd_{0.2}Fe_{11.8}Co_{0.2}O_{19}$ ferrite is less than −10 dB over the range of 9.8–18 GHz (1.5–3 mm in thickness).

As shown in Fig. 11, the measured reflection loss of $Sr_{0.8}Nd_{0.2}Fe_{11.8}Co_{0.2}O_{19}$ ferrite at thickness $d = 1.9$ mm was compared with the calculated results. The shapes of both measured and theoretically calculated results are similar to the curve pattern and absolute values. However, there are still some differences between the measured and calculated reflection loss. The minimum reflection loss at 15.4 GHz is nearly −16 dB for the measured results while the minimum reflection loss of −22 dB can be obtained at 16.2 GHz for the calculated results. The difference between the calculated and measured values can be attributed to the surface irregularity of absorber samples, the differences in the actual thickness of the layers, etc. [38].

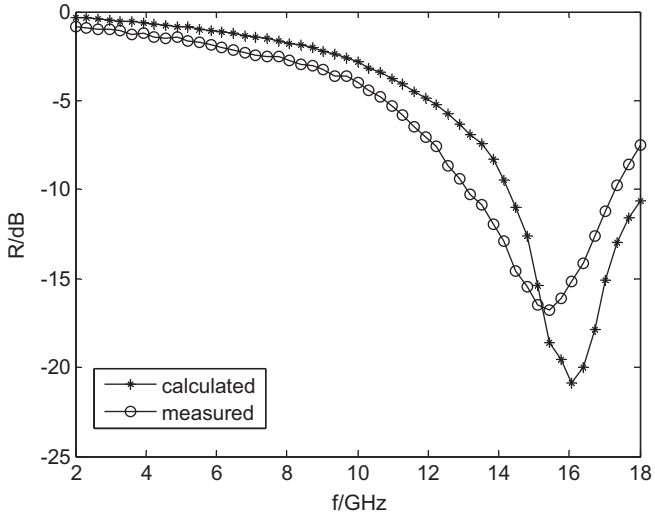

Fig. 11. Comparison between measured and calculated reflection loss for $Sr_{0.8}Nd_{0.2}Fe_{11.8}Co_{0.2}O_{19}$ ferrite.

4. Conclusions

Structural, magnetic properties and microwave absorption properties of Nd–Co-substituted M-type strontium hexagonal ferrite for different compositions ($x = 0.0$–0.4) prepared via sol–gel-autocombustion method have been investigated. The following conclusion can be drawn from this effort. Single lattice structure of strontium ferrite can be obtained when the substitution amount $x \leq 0.3$. Nd^{3+} ions preferentially substitute Sr^{2+} ions, and Co^{2+} ions preferentially substitute Fe^{3+} ions in octahedral $4f_2$ site and 2a site. Nd–Co substituted can enhance M_s and H_c, and reach a minimum at $x = 0.2$. The microwave absorption properties are significantly improved compared with pure strontium ferrite, because of higher dielectric loss induced by Co^{2+}, which partially substitutes Fe^{3+}. When the Nd–Co substitution amount $x = 0.2$, the minimum reflection loss is −22 dB, and the reflection loss is less than −10 dB over the range of 9.8–18 GHz (1.5–3 mm in thickness).

References

[1] W.B. Yang, Y.Y. Fu, A. Xia, K. Zhang, Z. Wu, J. Alloys Compd. 518 (2012) 6–10.
[2] V.K. Singh, A. Shukla, M.K. Patra, L. Saini, R.K. Jani, S.R. Vadera, N. Kumar, Carbon (2012), doi:10.1016/j.carbon.2012.01.033.
[3] S.H. Hosseini, S.H. Mohseni, A. Asadnia, H. Kerdari, J. Alloys Compd. 509 (2011) 4682–4687.
[4] W. Chen, J. Zhen, Y. Li, J. Alloys Compd. 513 (2012) 420–424.
[5] Z. Ma, Y. Zhang, C.T. Cao, J. Yuan, Q.F. Liu, J.B. Wang, Physica B 406 (2011) 4620–4624.
[6] R. Han, X.H. Han, L. Qiao, T. Wang, F.H. Li, Mater. Chem. Phys. 128 (2011) 317–322.
[7] G. Liu, L.Y. Wang, G.M. Chen, S.C. Hua, C.Q. Ge, H. Zhang, R.B. Wu, J. Alloys Compd. 514 (2012) 183–188.
[8] L. Vovchenko, L. Matzui, V. Oliynyk, V. Launetz, F. Le Normand, Physica E (2011), doi:10.1016/j.physe.2011.10.018.
[9] P. Saini, V. Choudhary, B.P. Singh, R.B. Mathur, S.K. Dhawan, Synth. Met. 161 (2011) 1522–1526.
[10] A. Maqsood, K. Khan, J. Alloys Compd. 509 (2011) 3393–3397.
[11] K. Shimba, N. Tezuka, S. Sugimoto, Mater. Sci. Eng. B: Solid 177 (2012) 251–256.
[12] Y.B. Feng, T. Qiu, J. Alloys Compd. 513 (2012) 455–459.
[13] Ashima, S. Sanghi, A. Agarwal, Reetu, J. Alloys Compd. 513 (2012) 436–444.
[14] M.K. Tehrani, A. Ghasemi, M. Moradi, R.S. Alam, J. Alloys Compd. 509 (2011) 8398–8400.
[15] C.A. Stergiou, G. Litsardakis, J. Alloys Compd. 509 (2011) 6609–6615.
[16] M.J. Iqbal, S. Farooq, Mater. Res. Bull. 46 (2011) 662–667.
[17] X.J. Gao, Y.C. Du, X.R. Liu, P. Xu, X.J. Han, Mater. Res. Bull. 46 (2011) 643–648.
[18] W. Onreabroy, K. Papato, G. Rujijanagul, K. Pengpat, T. Tunkasiri, Ceram. Int. 38S (2012) S415–S419.
[19] C. Serletis, G. Litsardakis, E.K. Polychroniadis, K.G. Efthimiadis, J. Alloys Compd. (2012), doi:10.1016/j.jallcom.2012.01.055.
[20] C.J. Li, B. Wang, J.N. Wang, J. Magn. Magn. Mater. 324 (2012) 1305–1311.
[21] P.G. Bercoff, C. Herme, S.E. Jacobo, J. Magn. Magn. Mater. 321 (2009) 2245–2250.
[22] C.A. Herme, P.G. Bercoff, S.E. Jacobo, Physica B (2011), doi:10.1016/j.physb.2011.12.036.
[23] Y. Liu, M.G.B. Drew, Y. Liu, J.P. Wang, M.L. Zhang, J. Magn. Magn. Mater. 322 (2010) 3342–3345.
[24] R.D. Shannon, Acta Crystallogr. A 32 (1976) 751.
[25] T. Kikuchi, T. Nakamura, T. Yamasaki, et al., J. Magn. Magn. Mater. 322 (2010) 2381–2385.
[26] G. Litsardakis, I. Manolakis, C. Serletis, K.G. Efthimiadis, J. Magn. Magn. Mater. 316 (2007) 170–173.
[27] G. Litsardakis, I. Manolakis, C. Serletis, K.G. Efthimiadis, J. Magn. Magn. Mater. 310 (2007) 884–886.
[28] L. Lechevallier, J.M. Le Breton, J.F. Wang, J. Phys.: Condens. Matter 16 (2004) 5359–5376.
[29] A. Morel, J.M. Breton, J. Kreisel, G. Wiesinger, F. Kools, Tenaud, J. Magn. Magn. Mater. 24 (2002) 242–245.
[30] X. Liu, P. Hernandez-Gmez, K. Huang, S. Zhou, et al., J. Magn. Magn. Mater. 305 (2006) 524–528.
[31] X. Liu, W. Zhong, S. Yang, Z. Yu, B. Gu, Y. Du, J. Magn. Magn. Mater. 238 (2002) 207.
[32] M.Z. Wu, Y.D. Zhang, S. Hui, T.D. Xiao, S.H. Ge, W.A. Hines, J.I. Budnick, G.W. Taylor, Appl. Phys. Lett. 23 (2002) 4404.
[33] Y.J. Kim, S.S. Kim, J. Electroceram. 24 (2009) 314–318.
[34] G.H. Jonker, H.P.J. Wijn, P.B. Braun, Philips Techn. Rev. 18 (1956–1957) 145.
[35] Y. Naito, K. Suetake, IEEE Trans. Microwave Theory Tech. 19 (1971) 65–72.
[36] M.R. Meshram, N.K. Agrawal, Bharoti Sinha, P.S. Misra, J. Magn. Magn. Mater. 271 (2004) 207–214.
[37] B.S. Zhang, Y. Feng, J. Xiong, Y. Yang, H.X. Lu, IEEE Trans. Magn. 42 (2006) 1778–1781.
[38] Y.C. Qing, W.C. Zhou, F. Luo, D.M. Zhu, J. Magn. Magn. Mater. 323 (2011) 600–606.